Rankine Cycle Efficiency Increase by the Regenerative Recovery of Historically Rejected Heat_rev1

by
Johan Enslin

Heat Recovery Micro Systems

Heidelberg
South Africa

Abstract:

Steam extraction from Rankine cycle turbines in order to heat the high pressure boiler water in a series of feedheaters, is common practice to increase the thermodynamic efficiency of cycles. Regenerative Cycles are so formed, which form the basis of most modern power generation rankine cycles used by electricity utilities globally.

By utilizing absorption heat transformer (AHT) principles, thermal powered hybrid heatpumps have been developed recently, making it possible to use these heatpumps for reclaiming rejected heat from rankine condensers for providing the required energy for feedwater heating, allowing additional power to be generated from the (historically used) extract steam, without requiring more heat to be added in the boiler. Cycle efficiency is therefore increased.

As the AHT-Hybrid heat transformer type heatpumps may generate higher temperatures than the boiler evaporation temperature in some lower temperature rankine cycles, the possibility exist that a much larger portion of the rejection heat in the condenser may be recovered and re-used regeneratively in the cycle. This enhanced regeneration give rise to the extremely high thermodynamic efficiency achieved by the REHOS Power Cycle.

These heat of solution (HOS) heat transformers, can practically only be used within limited temperature ranges, depending on critical temperature and pressure parameters of the binary media mixtures used eg. NH3-in-Aqua may be practical only between -30°C and +140°C making it ideal for ORC systems used eg. for geothermal power generation.

Introduction: Equation Chapter (Next) Section 1

The steam engine has been with us for over 100 years now, and utilizes the well-known Rankine cycle, as sketched on the Temperature-Entropy (T-S) Diagram of figure 1 below. A feedpump is used to increase the pressure of water in moving from (A) to (B) and the water is evaporated at constant temperature and pressure along line (B - C), where all the water is vaporized at (C). The saturated steam is then superheated along line (C - D) before entering the turbine, generating power as the HP steam expand isentropically following line (D - E). Note that the isentropic expansion line (D - E) cross the water-steam saturation line, implying the low pressure and temperature spent steam at point (E) contain a certain percentage liquid droplets in the turbine exhaust.

Figure 1
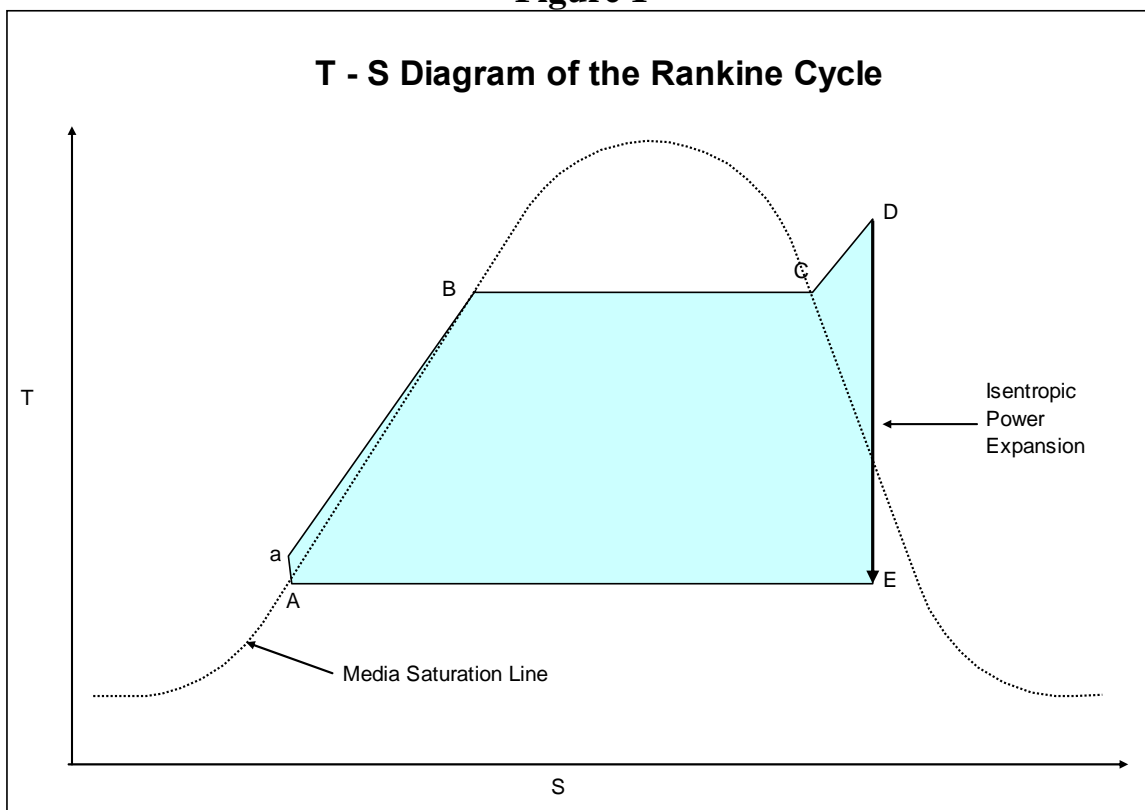
Heat is added to the cycle in water heating, ($Q_{heating}$) the HP water along line (A - B). More heat is added to evaporate the liquid, (Q_{evap}) along line (B - C), while a third amount of heat is added (Q_{sht}) along line (C - D), to superheat the saturated steam. After the power expansion work (W_{power}) done by the cycle along line (D - E), the remaining latent heat in the low pressure exhaust steam is rejected (Q_{rej}) out of the cycle by water cooled condensing along line (E - A). The power developed by the cycle is represented by the total enclosed (blue) area in figure 1, and heat rejection may be judged by the length of line (E - A) on the diagram. The thermodynamic cycle efficiency is given by:

$$\eta_{rankine} = \frac{W_{power}}{(Q_{heating} + Q_{evap} + Q_{sht})} \qquad (1.1)$$

and because the sum of all energy entering (+) and leaving (-) the cycle add to zero:

$$Q_{input} = (Q_{heating} + Q_{evap} + Q_{sht}) = W_{power} + Q_{rej} \qquad (1.2)$$

$$\eta_{rankine} = \frac{W_{power}}{(W_{power} + Q_{rej})} \qquad (1.3)$$

while it can be shown that the ideal, or Carnot efficiency of a heat engine operating between the same high temperature reservoir (T_{hot}), and low temperature reservoir (T_{cold}), is limited to a maximum of:

$$\eta_{carnot} = \frac{(T_{hot} - T_{cold})}{T_{hot}} \qquad (1.4)$$

Maximum (Carnot) efficiency would be attained when all heat input is done at a single high temperature, unlike the rankine cycle.

## Increasing Efficiency by Regenerative Feedheating

Modern power generation use the regenerative (or carnotized) cycle for higher efficiency. Partially expanded steam is extracted from the steam expanding in the turbine cascade at regular intervals and fed to feed water heaters, where it is condensed to use some latent energy from the expanding steam to raise the water temperature stepwise, before it reaches the boiler. This decrease the entropy of the expanding steam stepwise, to form a regenerative cycle as shown in the T - S diagram of figure 2 below. In the extreme, with numerous very small steps, the regenerative cycle diagram resembles a parallelogram, with the isentropic power expansion line (D - E) very nearly parallel to the water heating line (A - B), as the total heat given off by the expanding steam is added to the pumped feedwater in the feedheaters. This result in most heat added as (Q_{evap}) at the single evaporation temperature (T_{hot}), while heat rejection along line (E - A) also occur at the single temperature of the condenser (T_{cold}), with no external heat added to the cycle at different temperatures and therefore the efficiency of the cycle approaching carnot efficiency.

The higher efficiency is graphically visible in the length of the heat rejection line (E - A) of T - S diagram of the regeneration cycle in figure 2, compared to the length of line (E - A) of the rankine cycle T - S diagram in figure 1. The decrease in rejected heat (Q_{rej}) in the efficiency formula (1.3) may be used to calculate the efficiency of the regeneration cycle, and should the number of feedheaters in cascade be infinite, the cycle efficiency

would calculate to carnot efficiency. In practice the number of feedheaters vary from about 6 to 9, and the number is a trade-off between increased efficiency and the larger capital investment, maintenance and complexity of more feedheaters cascaded in the cycle.

Figure 3 below, show a typical example feedheater (LP-1) from a utility scale (500 MWe) coal-fired power station, being the first LP feed heater closest to the condenser, heated by steam from the last extract point of the LP turbine. Temperatures shown are those of the actual real power station.

Figure 2

T - S Diagram of the Regenerative Cycle
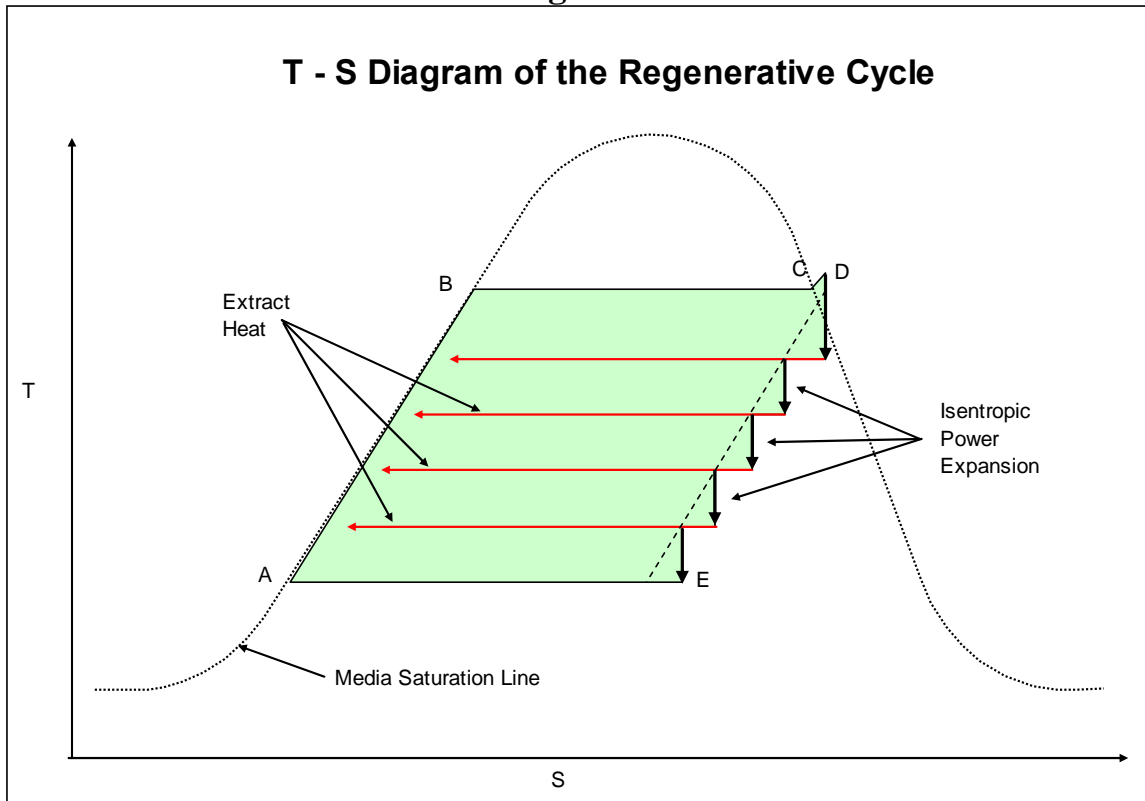
Note that the extract steam is at a (saturation) temperature of 68°C and therefore cannot heat the pumped water to a higher temperature than a small approach temperature some 2°C lower than this supply steam temperature. The heater liquid output heated temperature is thus 66°C. Looking at the regenerative cycle diagram of figure 2, it means that the regenerative heating as used commercially historically cannot quite reach the boiler temperature at point (B), and therefore cannot reach the ideal carnot efficiency.

The only way to change that, is by employing heatpumps to "upgrade" the temperature in each heater. A heatpump is sketched in on the diagram of figure 4 below, but although it may be used to achieve higher heater output temperatures, the temperatures in this schematic was kept the same as those of figure 3, specifically so we may evaluate the performance realistically by comparison.

Heatpump Utilization to avoid Extract Steam

We note that the heatpump installation, pump heat from the lower temperature (condenser) and use that to heat the feedwater in the feedheater. No extract steam from the turbine is required for this process, and the idea is that the additional power that may be developed in the turbine as a result of utilizing the formerly used extract steam for generating additional power, should ideally be more than the energy required for powering the heatpump.

Figure 3
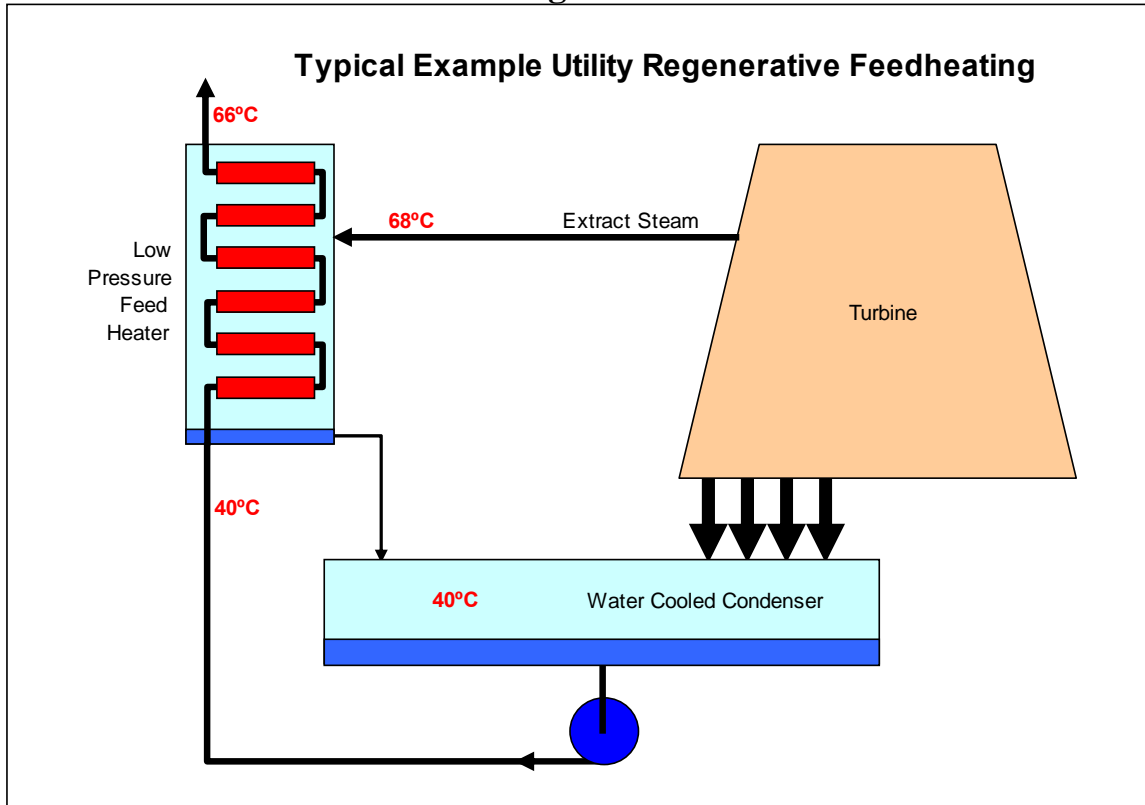
We assumed (at first) a standard vapor compression (VC) type heatpump using anhydrous NH3 as medium. For the heatpump to absorb heat from the condenser at 40°C, it would be required for the heatpump evaporator to operate at a temperature lower by a few degrees, so we assumed the evaporator would operate on 35°C. For similar reasons, the heatpump hot condenser (heat output), would have to operate on 73°C, making the saturated NH3 vapor pressure in the evaporator 13.7 Bar Abs, while the condenser would run at 35.9 Bar Abs. With a compressor isentropic efficiency of 75%, the power needed would be 185.2 kWe/kg NH3 used, and the heat delivered at 73°C per kg NH3 used calculate to 919.6 kW_th. The efficiency is represented by the coefficient of performance (COP) calculated as:

$$COP_{VC-Heatpump} = \frac{HeatPumped}{PowerUsed} = \frac{Q_{heat}}{W_{comp}} = 4.97 \qquad (1.5)$$

The ideal heatpump performance (delivering heat) is calculated using temperatures again:

$$COP_{carnot} = \frac{T_{hot}}{(T_{hot} - T_{cold})} = 9.11 \qquad (1.6)$$

Interesting to note that the actual VC Heatpump COP is therefore only 54.5% Carnot, as a result of mainly the required increased temperature delta to guarantee heat inflow into the evaporator and outflow from the condenser, as well as the low compressor isentropic efficiency.

The mass of extract steam from the turbine, that would have been required to deliver the same amount of heat as the VC-Heatpump (using 1 kg/s NH3 flow), namely 919.6 kW_th can be calculated as:

$$M_{extract} = \frac{HeatDelivered}{Enthalpy\_of\_Conden\sin g} = \frac{919.6kW}{(H_{vapor} - H_{liquid})} = 0.8404 kg / s \qquad (1.7)$$

and for this mass of steam expanding further down to condenser pressure in the turbine with an assumed 80% isentropic efficiency, the power developed would calculate to 121.37 kWe, which is only 65.5% of the power used by the heatpump compressor!

Figure 4

Utilizing Heatpumps for Regenerative Feedheating

The standard VC type heatpump can therefore not be used for this purpose, as it uses too much electrical power! We would have to explore heatpumps that use much less electrical power, and combine it with thermal energy for powering the heatpump.
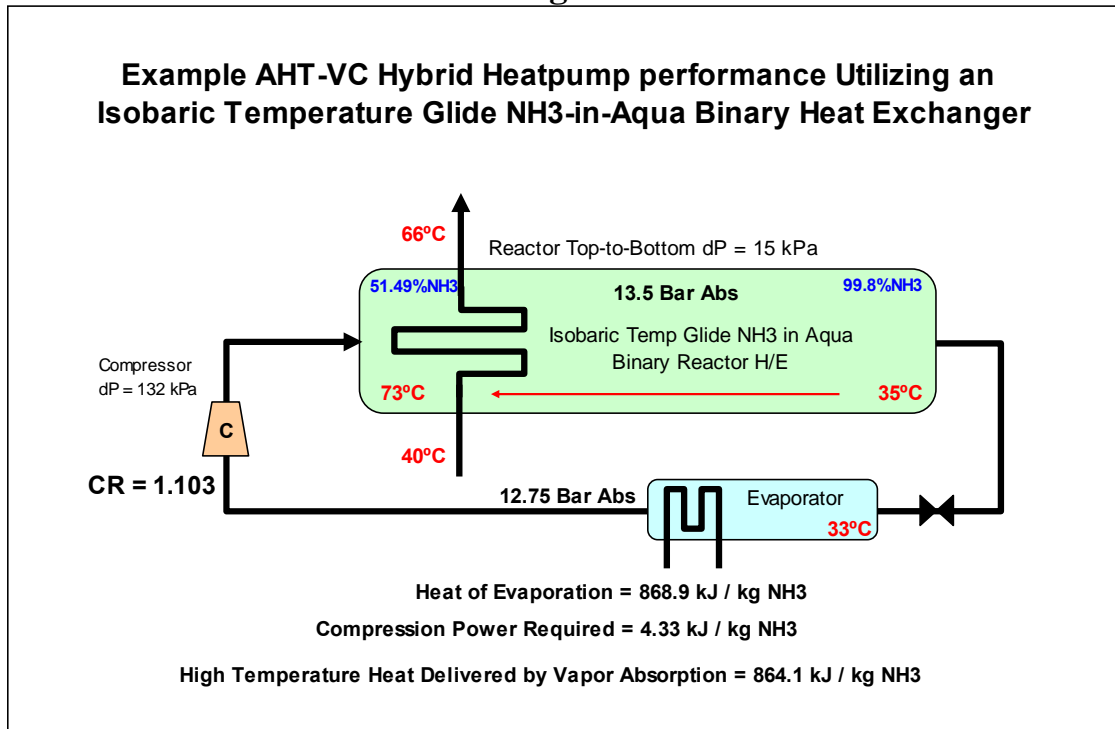
Development of Heat Transformer Type Heatpumps

An absorption heat transformer (AHT) work on the principles of using intermediate temperature heat (low temperature) to generate vapor in an evaporator, which is then absorbed into a suitable higher temperature absorber, to release the latent heat in the vapor as well as the heat of solution (HOS) of the vapor media into the absorber liquid media to raise the temperature. Temperature "upgrade" or "lift" typically range from 30°C to 80°C in a single stage AHT, depending on the actual binary media combination used. The AHT use mainly thermal energy ($Q_{thermal}$) to generate vapor, and then additionally use a small portion of the total heatpump energy requirement as electrical energy (W_{comp}) to either increase the vapor pressure to the absorber level, or use liquid pumping to increase the pressure to the evaporator prior to evaporation. The AHT used as heatpump would therefore have an efficiency calculated as COP of:

$$COP_{AHT} = \frac{Q_{pumped}}{(Q_{thermal} + W_{comp})} \qquad (1.8)$$

The compressor power used is a direct function of the compression ratio, so decreasing this compression ratio drastically, also decrease the electrical power consumed by the AHT.

Figure 5

Example AHT-VC Hybrid Heatpump performance Utilizing an Isobaric Temperature Glide NH3-in-Aqua Binary Heat Exchanger

66°C

Reactor Top-to-Bottom dP = 15 kPa

51.49%NH3   13.5 Bar Abs   99.8%NH3

Isobaric Temp Glide NH3 in Aqua Binary Reactor H/E

73°C   35°C

Compressor dP = 132 kPa

40°C

C

CR = 1.103

12.75 Bar Abs   Evaporator   33°C

Heat of Evaporation = 868.9 kJ / kg NH3

Compression Power Required = 4.33 kJ / kg NH3

High Temperature Heat Delivered by Vapor Absorption = 864.1 kJ / kg NH3

The Isobaric Temperature Glide Binary Reactor H/E

A typical AHT-VC Hybrid heatpump with the same temperature lift to replace the standard VC heatpump mentioned above is sketched in figure 5 above. Note the very low compression ratio required by this heatpump as a result of utilizing a binary isobaric temperature glide heat exchanger, where the differential pressure is the hydraulic liquid column (2 meter column height was assumed) under gravity pressure of 15 kPa only. The total compressor differential pressure amount to 132 kPa when the accumulated piping pressure drops are also added in.

Although the COP value is actually quite low and calculate to ~1 only, the electrical portion of the heatpump powering energy calculate to only 4.33 kJ/kg NH3 to power the compressor, as the thermal energy to drive the heatpump account for the balance of the total energy utilized for pumping heat! The low electrical power requirement make this type of regeneration in feed-heating concept a reality! The temperature-entropy diagram for this example heatpump would typically look like the sketch in figure 6, below.
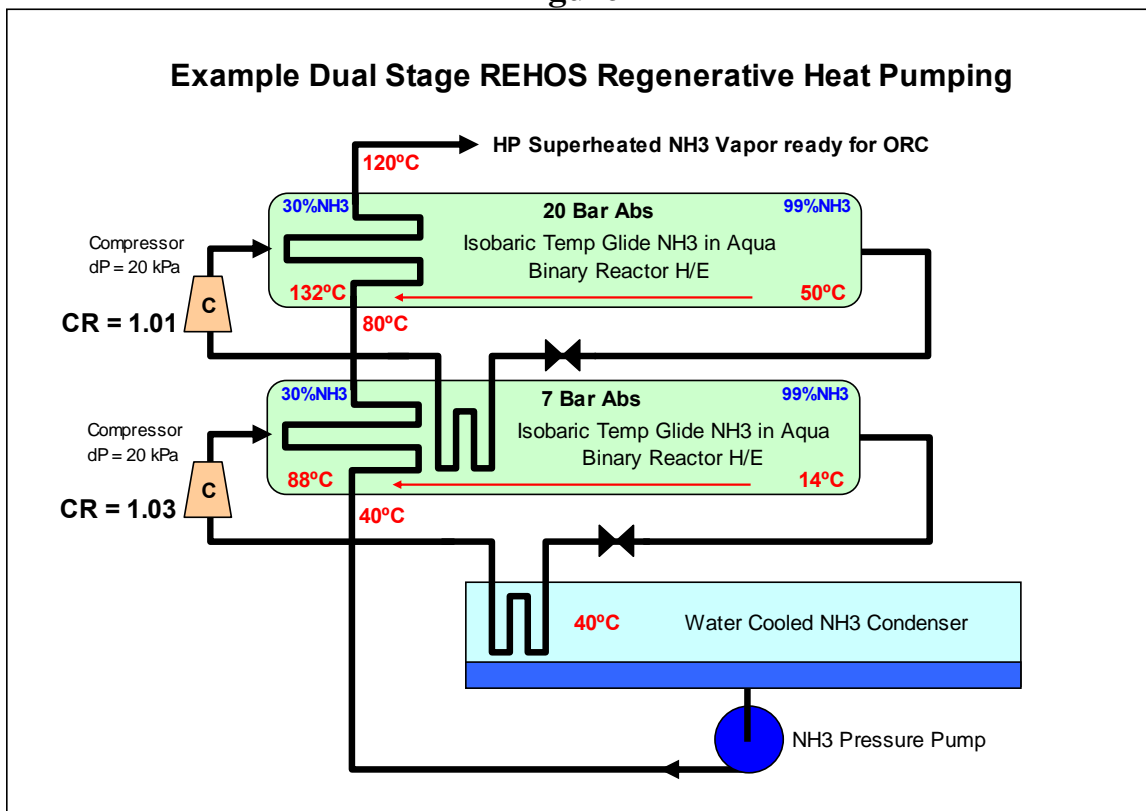
Figure 6
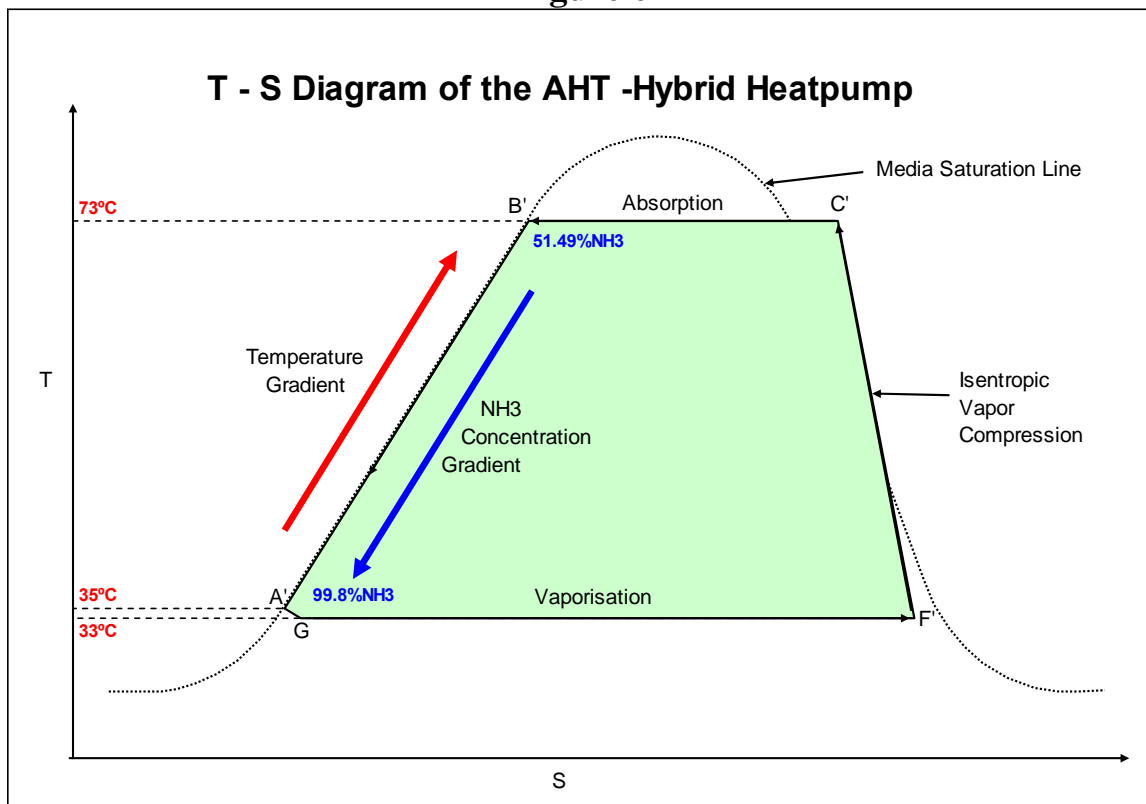
The same heat of solution (HOS) type hybrid heatpumps may easily be cascaded for larger overall temperature gains, as a single stage temperature gain would be limited to the 60 - 80°C lift only. A typical low temperature cascade is shown in the sketched diagram of figure 7 below. Another limitation of this heatpump cascade integration is brought about by the requirement of a zeotropic binary mixture capable of isobaric

temperature glides, at the proposed operating temperatures. Several different media-pairs are already known among various researchers, but for the NH3-in-Aqua mixture, the temperature upper limit would be around 130 - 140°C while the lower limit would be around -20°C to -30°C. This will allow HOS type heatpumps to be utilized replacing the standard feedheaters operating on extraction vapor, but only if the power generation cycle stays within the limitation of the upper and lower temperatures for it's feed heating heatpumps. For lower temperatures (below 140°C eg in geothermal heat recovery use) the organic rankine cycle (ORC) would easily form a Regenerative Heat of Solution (REHOS) cycle with very interesting characteristics. This cycle is achieved by integrating the AHT type heatpump sub-cycle regeneratively with an ORC sub-cycle in order to achieve a very high efficiency machine to generate power.

Figure 7

Example Dual Stage REHOS Regenerative Heat Pumping

When integrating the AHT type heatpump shown on the T - S Diagram of figure 6, regeneratively with the rankine (ORC) sub-cycle as shown on the T - S Diagram of figure 1, above, we can display it graphically in the T - S Diagram sketched in figure 8, below. Note that the media used in the heatpump may differ from the media used by the ORC, as shown in figure 8, and in this case the media does not mix. The media for the ORC may thus be chosen for the most efficient refrigerant for the operational temperatures and pressures best suited to the turbine, for the specific heat exchangers for heat input and heat reject, available. The heatpump media (unlike the ORC media) need to be a zeotropic binary mixture able to provide isobaric temperature gliding at the intended operating temperatures of the heatpump.

Complete regeneration is achieved when all the input heat used by the ORC is supplied via the ORC heat exchanger from the heatpump hot absorber, and all ORC Reject heat is absorbed via the ORC Rejection heat exchanger into the heatpump evaporator. This can only be achieved when the heatpump absorber operate at a higher temperature than the ORC input heat required, as well as the heatpump cold evaporator operate at a lower temperature than the ORC heat rejection temperature to guarantee proper heat inflow and outflow from the ORC, respectively.

Assuming a turbine with 70% isentropic efficiency, using pure NH3 as operating medium, the pressure at 66°C would be 30.6 Bar Abs, while the low pressure would be 15.8 Bar Abs at a saturation temperature of 40°C. The resulting ORC efficiency calculate to a netto efficiency of 4.4%, which represent a value of about 58% Carnot.

Figure 8
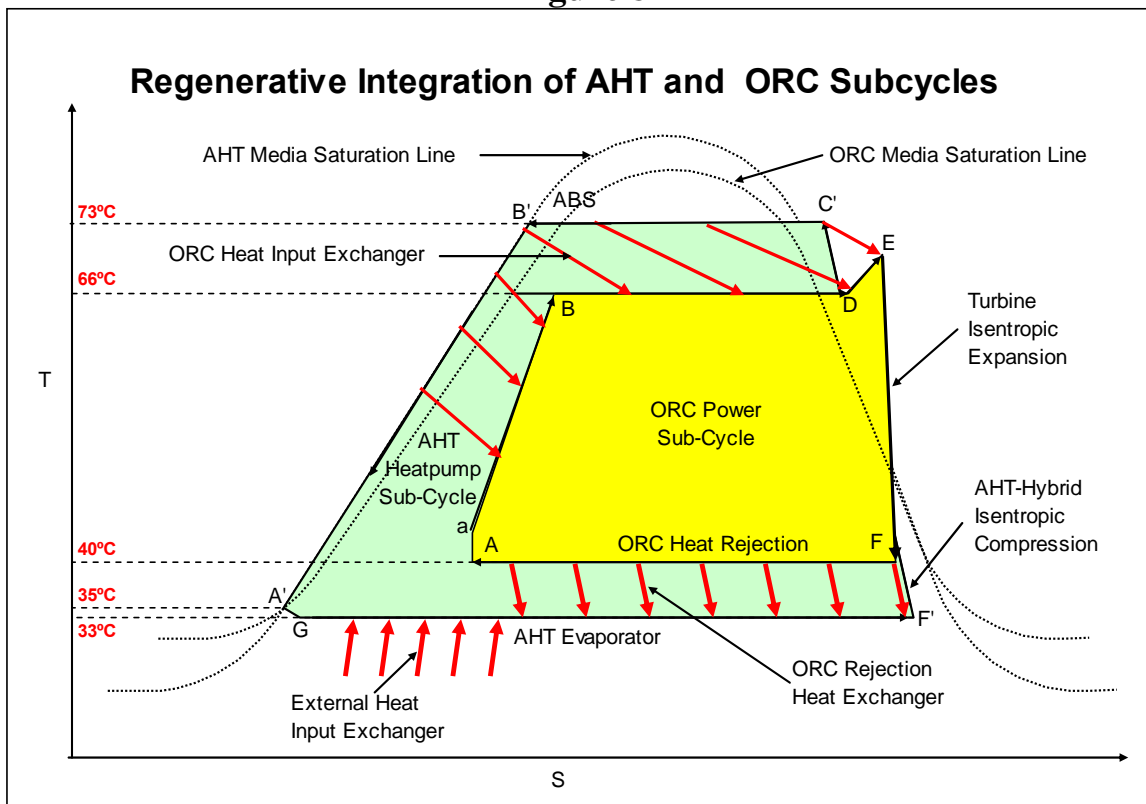
The integrated T - S Diagram sketched in figure 8, above, try to show the heatpump sub-cycle (in green) interacting with the ORC (in yellow) via the red arrows representing the heat exchangers. All the heatpump heat is sourced from the evaporator (line G - F') and the pumped heat sink deliver this heat to the ORC.

The component layout sketch of figure 9, below, use the same identifier letters and may be easier to explain the fully regenerative interaction of the heatpump sub-cycle with the ORC.

Critical to the heatpump operation is the pseudo-isobaric temperature gliding bubble reactor containing a strong solution of the zeotropic binary mixture of NH3 in aqua. This reactor has a large diameter to facilitate both vapor bubble vertical upflow and lower concentration mixture downflow driven by buoyancy effects against gravity. This density driven counter current flows allow heat-, mass-, and species transfer with the resultant high ammonia concentration and low temperature at the reactor top and low ammonia concentration higher temperature at the bottom of the reactor.

Figure 9

Sketch of REHOS Cycle layout for the exergy based analysis
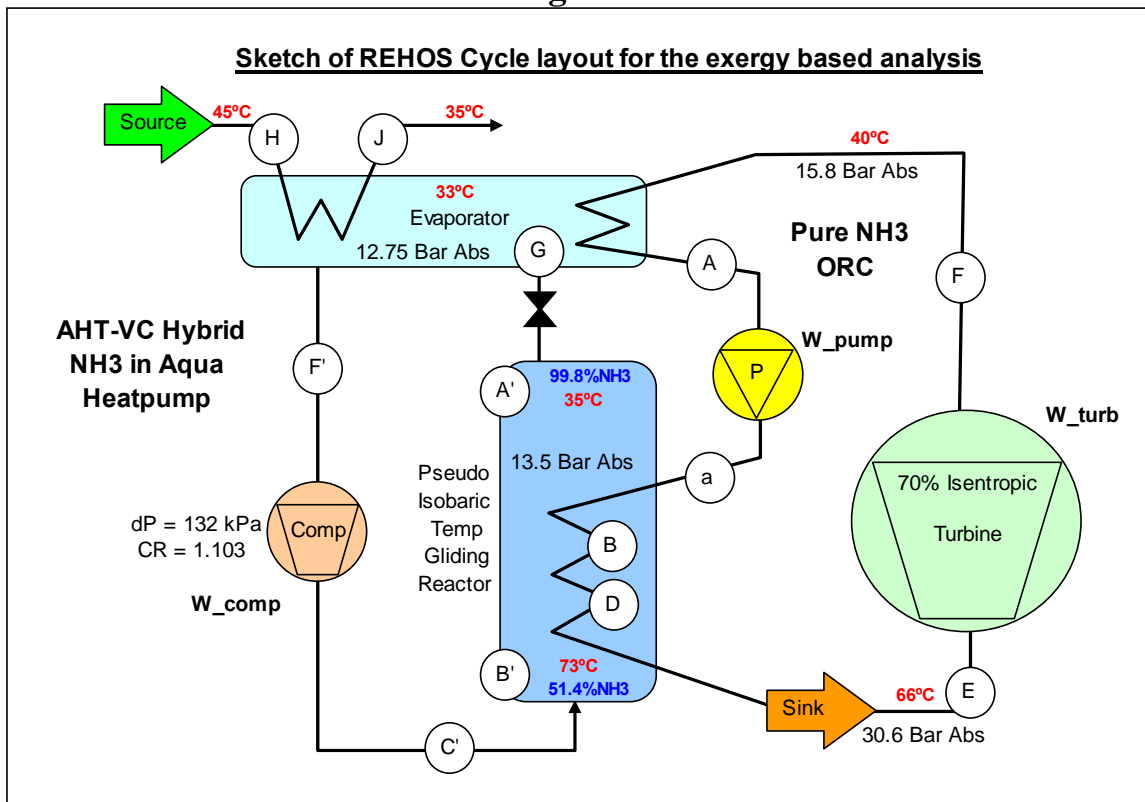
In operation the very rich liquid mixture (in this example 99.8% NH3 in aqua), flows from the reactor top end through the throttling valve into the evaporator with a slightly lower pressure (and 2°C lower temperature) where it is completely flashed into vapor, essentially isothermally. The small % water in this liquid is carried with the vapor to the compressor. Energy required for vaporising this liquid comes from both the waste heat source H/E coil (water flow H -> J) and the ORC heat rejection H/E coil (condensing flow F -> A).

Should we do an energy balance around the ORC and AHT cycles, we note the following state points of the alphabetically marked positions around the cycles:

Table 1

Position	Temp (Celsius)	Press (kPa)	Mass (kg/s)	Enthalpy (kJ/kg)	Entropy (kJ/kg.K)	Quality (x)	Media
A	40	1575	1.0	191.1	0.626	0%	NH3
a	40	3058	1.0	196.2	0.652	0%	NH3
B	66	3058	1.0	324.0	1.046	0%	NH3
D	66	3058	1.0	1286.6	3.884	100%	NH3
E	66	3058	1.0	1286.6	3.884	100%	NH3
F	40	1575	1.0	1231.9	3.968	94.71%	NH3

W_turbine =	54.7	kW		η_ORC =	4.4%		
W_pump =	5.1	kW		% Carnot =	57.0%		

We calculate the energy clockwise (ORC deliver energy) around the T - S Diagram following the convention that energy added to the cycle is positive and energy removed from the cycle is negative:

Condensate Pumping (A -> a) =>

$$W_{pump} = M.(H_a - H_A) = 5.1 \text{ kW} \tag{1.9}$$

Liquid heating (a -> B) =>

$$Q_{liquid\_heating} = M.(H_B - H_a) = 127.8 \text{ kW\_th} \tag{1.10}$$

Evaporation Heat (B -> D) =>

$$Q_{evap} = M.(H_D - H_B) = 962.6 \text{ kW\_th} \tag{1.11}$$

Total ORC Heat Input (a -> E) =>

$$Q_{heat} = M.(H_E - H_a) = 1090.3 \text{ kW\_th} \tag{1.12}$$

Turbine Power Delivered (E -> F) =>

$$W_{turbine} = M.(H_F - H_E) = \text{-54.7 kW\_e} \tag{1.13}$$

ORC Rejection Heat (F -> A) =>

$$Q_{rej} = M.(H_A - H_F) = \text{-1040.8 kW\_th} \tag{1.14}$$

Heat Balance (clockwise in delivering power) around ORC in the sequence =>

$$A \rightarrow a \rightarrow B \rightarrow D \rightarrow E \rightarrow F \rightarrow A$$

$$\sum_{CYCLE}^{ORC} Energy = W_{pump} + Q_{liquid\_heating} + Q_{evap} + W_{turbine} + Q_{rej} = 0 \qquad (1.15)$$

Similarly, state points are identified around the AHT-VC Hybrid heatpump and listed in table 2. Note that the mass column have been left blank for the two positions A' and B' because although the actual NH3 flow should be the same as C', F' and G, the reactor also contain a large mass of water. As vapor is absorbed (and heat produced) close to the bottom end of the reactor, the NH3-rich vapor bubbles and immediate bubble surrounding NH3-rich liquid will migrate upwards due to density differences, and the heated, NH3-lean liquid would migrate downwards. This counter-current internal circulation flow in the reactor facilitate mass-, heat-, and species transfer maintaining the temperature and NH3 concentration gradients typical of the isobaric temperature glide heat exchanger. Heat continuously being removed from the hot reactor bottom, as well as the internal liquid circulation described above, make the vapor absorbsion process nearly isothermal.

Table 2

Position	Temp (Celsius)	Press (kPa)	Mass (kg/s)	Enthalpy (kJ/kg)	Entropy (kJ/kg.K)	%NH3 (kg/kg)	Media
A'	35	1352		166.6	0.568	99.80%	NH3-H2O
B'	73	1357		89.9	1.064	51.49%	NH3-H2O
C'	39	1408	1.313	1030.7	4.273	99.80%	NH3-H2O
F'	33	1276	1.313	1026.4	4.230	99.80%	NH3-H2O
G	33	1276	1.313	166.6	0.575	99.80%	NH3-H2O
H	45	200	2.101	188.4	0.639	-	H2O
J	35	195	2.101	146.6	0.505	-	H2O

W_comp =	4.3 kJ/kg	Electrical COP_e =	200
Q_heatpump =	162.2 kJ/kg	Thermal COP_th =	1.01
		Real Thermodynamic COP (~ 60%Carnot) =	5.19

The evaporator is also providing a nearly isothermal evaporation process as a result of the high NH3 concentration of the liquid entering the evaporator (99.8%NH3). The small amount of water is carried out with the NH3 vapor, to the vapor compressor.

Note that the heat transformer type heatpumps are powered mainly by thermal energy, as mentioned already. In table 2 the amount of thermal energy required to power this specific heatpump have been calculated and listed as $Q_{heatpump}$. If we assume the COP may be around 60% Carnot, it calculates to a value of 5.19 as listed in table 2. The actual amount of thermal energy may therefore be calculated: =>

$$COP_{heatpump} = \frac{Q_{pumped\_heat}}{(Q_{heatpump} + W_{comp})} = 5.19 \quad (1.16)$$

calculating to $Q_{heatpump}$ = 213 kW with the listed mass flow of M_{AHT} = 1.313 kg/s.

All input heat enter the AHT-VC Hybrid cycle in the evaporator along line (G - F').

$$Q_{heatpump\_input} = M_{AHT}.(H_{F'} - H_G) = 1128.5 \text{ kW\_th} \quad (1.17)$$

The heatpump compressor energy in line (F' -> C') calculate to: =>

$$W_{comp} = M_{AHT}.(H_{C'} - H_{F'}) = 5.65 \text{ kW\_e} \quad (1.18)$$

Vapor absorption in hot reactor bottom in line (C' -> B') =>

$$Q_{absorption\_heat} = M_{AHT}.(H_{B'} - H_{C'}) = -1234.9 \text{ kW\_th} \quad (1.19)$$

Absorbed NH3 moving down the isobaric temperature glide (B' -> A') =>

$$Q_{glide} = M_{AHT}.(H_{A'} - H_{B'}) = 100.7 \text{ kW\_th} \quad (1.20)$$

Leaving the heat exchanger, a small pressure drop across the throttling valve along line (A' -> G) would be isenthalpic, flashing a very small amount (~1%) of liquid into vapor as the mixture flow into the evaporator, dropping the temperature only 2°C in this process.

Heat balance around the AHT-VC Hybrid type heatpump sub-cycle (in anti-clock direction as the cycle absorb heat) in the sequence =>

$$\text{G -> F' -> C' -> B' -> A' -> G}$$

$$\sum_{CYCLE}^{AHT} Energy = Q_{heatpump\_input} + W_{comp} + Q_{absorption\_heat} + Q_{glide} = 0 \quad (1.21)$$

Integrating the two sub-cycles, it becomes clear the heat rejection energy from the ORC we called Q_{rej} has a large negative value, and would be totally absorbed into the heatpump evaporator, decreasing drastically the amount of external heat required to balance the energy around the heatpump cycle. As heat required by the heatpump flows into the heatpump (and is therefore calculated as positive values) the external heat absorbed into the evaporator may be calculated =>

$$Q_{external} = Q_{heatpump\_input} + Q_{rej} = 87.7 \text{ kW\_th} \quad (1.22)$$

as Q_{rej} is totally absorbed into the evaporator of the heatpump. Remembering that the heat used by the ORC is summed in formula (1.12) as:

$$Q_{heat} = 1090.3 \text{ kW\_th} \tag{1.23}$$

In this example the heat flow into the integrated two sub-cycles (REHOS Cycle) may be added up providing us with the complete energy balance of the REHOS cycle:

$$\sum_{CYCLE}^{REHOS} Heat = Q_{heatpump\_input} + W_{comp} + Q_{absorption\_heat} + Q_{glide} + W_{pump} + Q_{heat} + W_{turbine} + Q_{rej} = 0 \tag{1.24}$$

$$\sum_{CYCLE}^{REHOS} Heat = Q_{external} + W_{comp} + Q_{absorption\_heat} + Q_{glide} + W_{pump} + Q_{heat} + W_{turbine} = 0 \tag{1.25}$$

or written in real values:

$$\sum_{REHOS}^{CYCLE} Heat = (87.7) + (5.67) + (-1234.9) + (100.7) + (5.12) + (1090.3) + (-54.7) = \sim 0 \tag{1.26}$$

The only heat input into the cycle ($Q_{external}$ = 87.74 kW) comes from external sources and must be supplied by the Source thermal input.

This allow us to calculate the total REHOS Cycle first order energy efficiency : =>

$$\eta_{REHOS} = \frac{NettoPower}{HeatInput} = \frac{(-W_{turbine} - W_{comp} - W_{pump})}{Q_{external}} \tag{1.27}$$

$$\eta_{REHOS} = \frac{(54.66 - 5.12 - 5.67)}{87.74} = \mathbf{\color{red}{50.0\%}} \tag{1.28}$$

As the REHOS cycle essentially consist of 2 sub-cycles, namely a heatpump for which the ideal, Carnot COP may be calculated in terms of the Source temperature (T_c) and the Sink temperature (T_h) calculated in Kelvin (see also formula (1.6) on page 6): =>

$$COP_{carnot} = \frac{T_h}{T_h - T_c} \tag{1.29}$$

and an ORC for which the ideal, Carnot efficiency may be calculated in temperature terms as: =>

$$\eta_{ORC} = \frac{[(T_h - x) - (T_c + y)]}{(T_h - x)} \qquad (1.30)$$

which is the same formula that was provided (1.4) on page 3, but the ORC high temperature is lower than the heatpump Sink temperature (T_h), by x°C to allow heat to flow from the heatpump Sink to the ORC hot heat exchanger. Similarly, the ORC heat rejection must be at a temperature higher than the heatpump Source temperature (T_c) by y°C to allow heat to flow from the ORC heat exchanger into the heatpump Source (heatpump evaporator). In the example calculations above, x = 7°C and y = 7° C to be practical, with ($T_h = 73°C$) and ($T_c = 33°C$). The maximum (Carnot) efficiency of the REHOS cycle can therefore be calculated as: =>

$$\eta_{carnot} = [\frac{T_h}{(T_h - T_c)}].[\frac{\{(T_h - x) - (T_c + y)\}}{(T_h - x)}] \qquad (1.31)$$

and a few sample calculations was done and is presented in table 3 for illustration purposes.

Table 3

REHOS Maximum (Carnot) Cycle Efficiency				
T_h (Celsius)	T_c (Celsius)	x (Celsius)	y (Celsius)	Carnot Efficiency
73	33	7	7	66.3%
73	33	5	5	76.1%
73	33	2	2	90.5%
73	33	2	0	95.6%
73	33	0	0	100.0%
120	-30	7	7	92.3%
120	-30	5	5	94.5%
120	-30	2	2	97.8%
120	-30	2	0	99.2%

Should the values of x and y be reduced to zero, the Carnot efficiency calculate to 100% for the REHOS cycle maximum efficiency, but every heat exchanger need at least a small temperature differential to guarantee proper heat flow around the cycle. In the first line of table 3 the temperatures of this example REHOS cycle is represented, which means that the mass flow of medium in the heatpump sub-cycle set to be ($M_{AHT} = 1.313$ kg/s) for heat balance of the AHT-, ORC-, as well as the REHOS cycle would guarantee system efficiency less than Carnot efficiency! In this case some 4% of the ORC heat input (Q_{heat}) is un-usable and need to be dissipated (rejected) from the hot bubble reactor bottom, while the calculated REHOS cycle efficiency of 50% (see calculation in (1.28) above), correspond to the realistic ~ 79% of the Carnot value listed in table 3.

As expected, table 3 also show that the higher the temperature span between Source and Sink, the higher the maximum cycle efficiency, and obviously the smaller the heat exchangers approach temperatures (x and y), the higher the maximum cycle efficiency.

Although the example REHOS cycle analysed above has a thermodynamic efficiency of 50%, optimizing the design for minimum heat exchanger approach temperatures and a more reasonable temperature span between Source and Sink would easily produce cycle efficiencies of 80% - 90% in utilization of very low temperature (below 50°C) waste heat to produce power.

Figure 10

T - S Diagram of the REHOS Cycle -Simplified
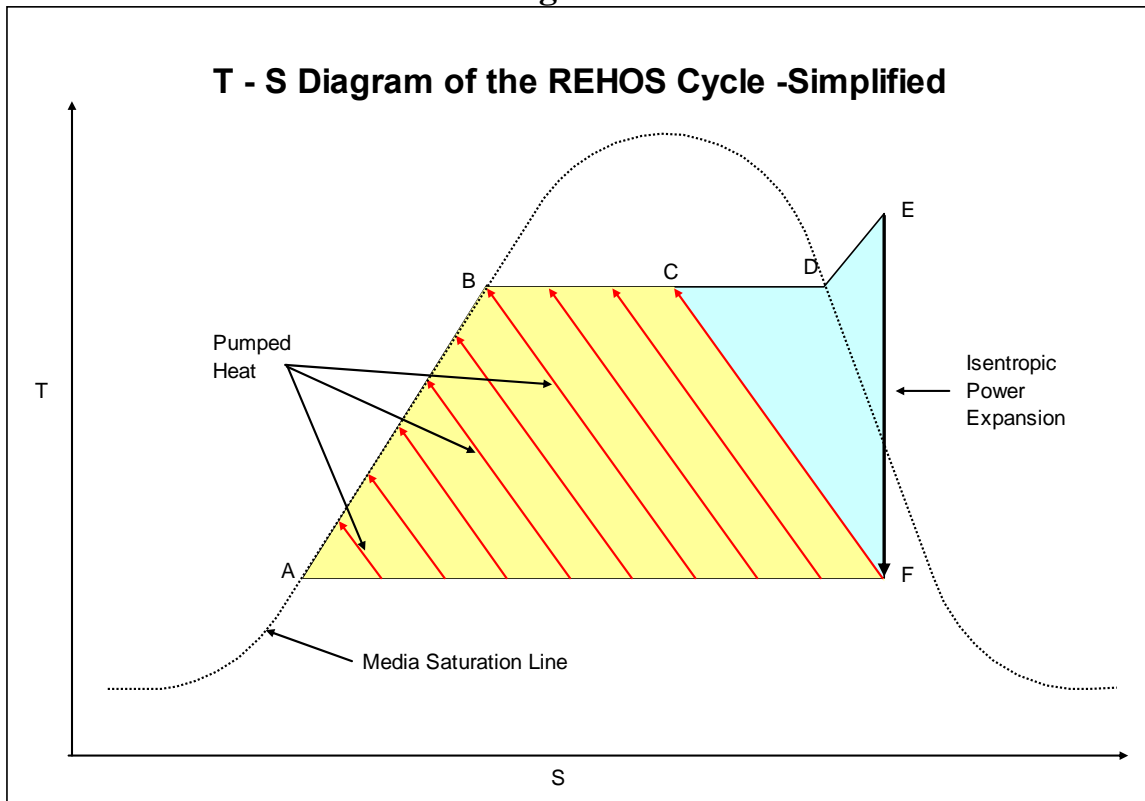
The vapor absorption process was already used extensively for years in absorption heat transformers (AHT's) for temperature lift, used for the economic temperature "upgrade" of very low temperature heat sources.

It is interesting to know that this high REHOS cycle efficiency is attained even though the ORC power sub-cycle have an efficiency of only 4.4%, but may be somewhat larger if we design the ORC sub-cycle to operate on a higher temperature delta. The ORC expander efficiency also have very little effect on the efficiency of the REHOS cycle, and the main (99%) of REHOS cycle inefficiency is due to thermal heat loss as a result of the non-perfect thermal insulation and irreversible heat transfer processes. The **secret of this high performance is the <u>large regenerative heat recovery</u> of the ORC heat rejection made possible by the absorption process in the isobaric temperature glide direct contact heat exchanger**.

As figure 9 is quite busy, we have redrawn a simplified version of the complete cycle as figure 10, above. In this example calculation presented in this paper, the external heat inflow need to come from a waste-heat source with a temperature some degrees above the 33°C heatpump evaporator temperature eg. an existing utility rankine cycle cooling system with the condenser operating on 45 - 48°C. With the REHOS Cycle, however, the cold end of the isobaric temperature glide heat exchanger may be chosen arbitrarily to suit the waste heat source temperature from which power need to be generated. It is not limited to the availability of low temperature cooling water, as the cycle heat rejection takes place at higher temperatures, so cooling water is not used and the REHOS cycle input heat evaporator may therefore easily be designed to operate at a lower temperature like 0°C to be able to extract ambient heat from the environment at 20 - 30°C.

Note that no cooling towers are required, as all the ORC reject heat is recycled by using the heatpump, and heat is rejected out of the cycle by thermal leakage from hot components only.

The high cycle efficiency, independent of actual temperature levels make the REHOS Cycle the perfect power generator for lower temperatures. It has immediate great value in low-grade heat recovery, even recovering heat from existing utility scale rankine cycles to generate a lot of power from the cooling circuits, re-using the reject heat from the condenser......

The uses of the REHOS technology is only limited by our small imagination!

In my previous publications (referenced below) I have comprehensively dealt with an AHT Hybrid heatpump design without vapor compressor in [14], while the paper [10] described the same hybrid heatpump, but this time using a vapor jet ejector as compressor. The publication [8] compared the VC type heatpump with various AHT-Hybrids and also introduce the HOS heatpump, as used in this current paper, while [7] clarify some conventions in calculation of COP's in heat powered heatpumps and heat transformers.

The referenced paper [13] describe the details of the isobaric temperature glide zeotropic binary reactor heat exchanger, and [3] clarify some of the process parameters used.

The actual REHOS Cycle introduction was done at a conference in South Africa in July 2017 with the introductory paper [1], which was subsequently followed by [2] as a simpler version of the same cycle.

Some of the numerous foreseen applications and use of REHOS technology was detailed in [5] and repeated more recently (April 2018) in the paper [11].

The publications [6], [9], [12] and [15] give an executive overview of the REHOS technology.

Previous Publications:

1. Paper presented at PowerGen Africa Conference July 2017 and published in the conference proceedings titled "Introducing a novel thermodynamic cycle (patent pending), for the economic power generation from recovered heat pumped from the huge global thermal energy reservoir called earth" by Johan Enslin, Heat Recovery Micro System CC. This paper is also accessible from my website http://www.heatrecovery.co.za/.cm4all/iproc.php/PowerGen-Africa 2017 Proceedings Speaker0_Session19149_1.pdf

2. A Paper titled "The Simplified REHOS Cycle.pdf" was written by Johan Enslin in August 2017 and published on my website http://www.heatrecovery.co.za/.cm4all/iproc.php/The Simplified REHOS Cycle.pdf

3. A Paper titled "Clarifying Process Parameters for the REHOS Cycle Concept_rev3.pdf" was written by Johan Enslin in October 2017 and published on [my website http://www.heatrecovery.co.za/.cm4all/iproc.php/Clarifying Process Parameters for the REHOS Cycle Concept_rev3.pdf](http://www.heatrecovery.co.za/.cm4all/iproc.php/Clarifying Process Parameters for the REHOS Cycle Concept_rev3.pdf)

4. The Paper titled "The Binary NH3-H2O Bubble Reactor_rev1.pdf" was written by Johan Enslin in December 2017, and published on my website http://www.heatrecovery.co.za/.cm4all/iproc.php/The Binary NH3-H2O Bubble Reactor_rev1.pdf

5. The Paper titled "The Competitive Advantages of REHOS Technology_rev1.pdf" was compiled by Johan Enslin in early January 2018, and published on my website http://www.heatrecovery.co.za/.cm4all/iproc.php/Competitive Advantages of REHOS Technology_rev1.pdf

6. Another paper, "Executive Overview of the REHOS Technology_rev1.pdf" was compiled by Johan Enslin in February 2018 and published on my website http://www.heatrecovery.co.za/.cm4all/iproc.php/Executive Overview of the REHOS Technology_rev1.pdf

7. The follow-up document "Clarification of COP calculations for Absorption Heat Transformer (AHT) Type Heat Pumps.pdf" was written by Johan Enslin (to enhance the Executive Overview paper) in March 2018 and published on my website http://www.heatrecovery.co.za/.cm4all/iproc.php/Clarification of COP calculations for Absorption Heat Transformer (AHT) Type Heat Pumps.pdf

8. The document titled "Comparison of various Modern Heatpump Technologies for unlocking Commercial Value from Ambient Heat_rev4.pdf" was written by Johan Enslin in April 2018 and published on my website http://www.heatrecovery.co.za/.cm4all/iproc.php/Comparison of various Modern Heatpump Technologies for unlocking Commercial Value from Ambient Heat_rev4.pdf

9. The document titled "Executive Overview of the REHOS Technology Redone April 2018.pdf" was written by Johan Enslin in April 2018 and published on my website http://www.heatrecovery.co.za/.cm4all/iproc.php/Executive Overview of the REHOS Technology Redone April 2018.pdf

10. The document titled "The Proof-of-Concept Model of the REHOS Ejector Heat Pump Part 1.pdf" was written by Johan Enslin in April 2018 and published on my website http://www.heatrecovery.co.za/.cm4all/iproc.php/The Proof-of-Concept Model of the REHOS Ejector Heat Pump_Part 1.pdf

11. The document titled "Competitive Advantages of REHOS Technology_rev2.pdf" was written by Johan Enslin in April 2018 and published on my website http://www.heatrecovery.co.za/.cm4all/iproc.php/Competitive Advantages of REHOS Technology_rev2.pdf

12. The document titled "REHOS Technology Executive Summary.pdf" was written by Johan Enslin in April 2018 and published on my website http://www.heatrecovery.co.za/.cm4all/iproc.php/REHOS Technology Executive Summary.pdf

13. The document titled "The Binary NH3-H2O Bubble Reactor -redone_rev2.pdf" was written by Johan Enslin in July 2018 and published on my website http://www.heatrecovery.co.za/.cm4all/iproc.php/The Binary NH3-H2O Bubble Reactor -redone_rev2.pdf

14. The document titled "The Syphon Bubble Reactor Heat Transformer as Heatpump in the REHOS Cycle_rev1.pdf" was written by Johan Enslin in July 2018 and published on my website http://www.heatrecovery.co.za/.cm4all/iproc.php/The Syphon Bubble Reactor Heat Transformer as Heatpump in the REHOS Cycle_rev1.pdf

15. The document titled "REHOS Cycle at a Glance August 2018.pdf" was written by Johan Enslin in August 2018 and published on my website http://www.heatrecovery.co.za/.cm4all/iproc.php/REHOS Cycle at a Glance August 2018.pdf

16. Website for Heat Recovery Micro Systems where the above publications are available from: www.heatrecovery.co.za